Presynaptic 5-HT1A is Related to 5-HTT Receptor Density in the Human Brain

Subrata K Bose*,[1,2,3], Mitul A Mehta[1,2,3], Sudhakar Selvaraj[1,4], Oliver D Howes[1,2,4], Rainer Hinz[5], Eugenii A Rabiner[2,6], Paul M Grasby[1,2], Federico E Turkheimer[1,2] and Venkatesha Murthy[1,2,6]

[1]PET Methodology, MRC-Clinical Sciences Centre, Imperial College London, Hammersmith Hospital Campus, London, UK; [2]Department of Medicine, Imperial College London, London, UK; [3]Department of Neuroimaging, Institute of Psychiatry, King's College London, London, UK; [4]Department for Psychosis Studies, Institute of Psychiatry, King's College London, UK; [5]Wolfson Molecular Imaging Centre, Manchester University, Manchester, UK; [6]GlaxoSmithKline Clinical Imaging Centre, Hammersmith Hospital, London, UK

5-Hydroxytryptamine (5-HT or serotonin) is an important neurotransmitter for a number of brain functions and widely distributed throughout the brain. Physiological and pharmacological relationship between 5-HT1A receptors and serotonin transporter (5-HTT) in the regulation of 5-HT neurotransmission has now been documented. A relationship between 5-HT1A receptors and 5-HTT is also suggested by the pathophysiology of depression and the mechanism of action of antidepressants. We have scanned 42 healthy adults with both [11C] WAY-100635 and [11C] DASB to investigate the anatomical co-distribution of multiple serotonergic markers. We hypothesized that lower 5-HTT densities in the dorsal raphe nucleus (DRN) and limbic regions will be accompanied by lower 5-HT1A receptor density in the same regions, contributing to the 5-HT1A receptor desensitization. In addition, variations in DRN 5-HT1A receptor density can theoretically influence the density and/or function of other serotonin receptor subtypes and the 5-HTT consequent to changes in serotonergic tone. In a comparatively large sample of volunteers, we have shown that the relationship between 5-HT1A and 5-HTT PET indices was complex. We were unable to demonstrate robust, intra-regional relationships between 5-HT1A and 5-HTT densities. Inter-regionally, DRN 5-HT1A receptors were related to cortical (temporal and frontal regions) and paralimbic (insula), but not limbic 5-HTT. This latter finding may reflect differences in 5-HT tone between individuals, and highlights probable substrates sensitive to variations in DRN 5-HT function.
Neuropsychopharmacology (2011) **36**, 2258–2265; doi:10.1038/npp.2011.113; published online 13 July 2011

Keywords: 5-HT1A; 5-HTT; antidepressants; drug discovery; PET; serotonin

INTRODUCTION

5-Hydroxytryptamine (5-HT or serotonin) neurons are widely distributed throughout the brain, and dysfunction in the serotonergic system is associated with a number of disorders, including depression, anxiety, chronic fatigue syndrome, and schizophrenia (Abi-Dargham, 2007; Cleare et al, 2005; Cowen, 2008; Geyer and Vollenweider, 2008).

Serotonin cell bodies are clustered in the mesencephalon and densely located in the dorsal raphe nucleus (DRN). 5-HT cell bodies in the DRN send projection fibers throughout the forebrain to limbic, striatal, and cortical regions. Both 5-HT1A and serotonin transporters (5-HTT) are positioned to have a key role in maintaining 5-HT

*Correspondence: Dr SK Bose, PET Methodology, MRC-Clinical Sciences Centre, Imperial College London, Hammersmith Hospital Campus, Du Cane Road, London W12 0NN, UK, Tel: +44 (0) 208383 3725, Fax: +44 (0) 208383 1783,
E-mail: subrata.bose@imperial.ac.uk

homeostasis due to their location on presynaptic 5-HT neurones (Barnes and Sharp, 1999) and on 5-HT projection sites (Kish et al, 2005; Varnäs et al, 2004). 5-HT1A receptors are present both as somatodendritic autoreceptors on 5-HT cell bodies in the midbrain and brainstem; and as postsynaptic (or heteroreceptors) receptors in 5-HT projection areas. 5-HTT, present on DRN cell bodies, terminal dendrites, and axons, terminate 5-HT neurotransmission by their high-affinity reuptake of released synaptic 5-HT (Hoyer et al, 2002; Barnes and Sharp, 1999).

It is now accepted that there is a physiological and pharmacological relationship between 5-HT1A receptors and 5-HTT in the regulation of 5-HT neurotransmission (Alexandre et al, 2006; Fox et al, 2010; Gobbi et al, 2001; Li et al, 2000; Mannoury la Cour et al, 2001). For example, 5-HTT knockout mice have region-specific changes in the adult 5-HT1A receptor density with reductions in dorsal raphe, hypothalamus, and amygdala, but increased or unchanged densities in the hippocampus (Alexandre et al, 2006; Li et al, 2000; Mannoury la Cour et al, 2001) and no changes in entorhinal and frontal cortices. Similarly, mice

expressing lower DRN 5-HT1A autoreceptors have increased raphe cell firing rates and larger increases in serotonin levels when administered the selective serotonin reuptake inhibitor (SSRI) fluoxetine, measured in the hippocampus and prefrontal cortex (Richardson-Jones et al, 2010).

What is not clear from these studies is whether specific associations of 5-HT1A receptor and 5-HTT densities may also be detectable within normal human populations. In addition, variations in DRN 5-HT1A receptor density can theoretically influence the density and/or function of other serotonin receptor subtypes and the serotonin transporter (5-HTT) consequent to changes in serotonergic tone (Richardson-Jones et al, 2010). Anatomical co-distribution of multiple serotonergic markers can be studied in vivo in the human brain using PET imaging (Frey et al, 2008; Lundberg et al, 2007; Takano et al, 2008). Indeed, a significant positive linear association between 5-HT1A receptor density indexed using [11C] WAY-100635 and 5-HTT binding indexed using [11C]MADAM has been shown in the brainstem raphe and hippocampus, but not the frontal cortex in a group of 12 volunteers (Lundberg et al, 2007). In an exploratory analysis, in a group of 17 male volunteers (Takano et al, 2008) showed negative linear associations between [11C] WAY-100635 BP_{ND} and [11C] DASB BP_{ND} (for 5-HTT) in the cingulate, insula, frontal, lateral temporal, and parietal cortices. In an attempt to resolve these inconsistencies, we have scanned 42 healthy adults with both [11C] WAY-100635 and [11C] DASB. We hypothesized that 5-HTT densities in the DRN and limbic regions will be related to 5-HT1A receptor density in the same regions. Given the recent suggestion that these relationships may be nonlinear based on the studies of 5-HT2A and 5-HTT receptor densities (Erritzoe et al, 2010), we tested both linear and 2nd and 3rd order polynomial relationships. In addition to our prediction that there will be intra-regional correlations in 5-HTT and 5-HT1A receptor densities in the DRN and limbic areas, we predicted that raphe 5-HT1A receptor density would be related to cortical 5-HTT density due to the variations in 5-HT levels (tone) predicted by 5-HT1A density in the DRN (Richardson-Jones et al, 2010). All volunteers were also genotyped for the 5-HTTLPR to explore possible modulating influences of genetic variations.

MATERIALS AND METHODS

Participants

Forty-two healthy adult male volunteers (mean age = 38 years; SD = 11 years; range = 25–60 years) were included in this study. None of the participants met Diagnostic and Statistical Manual of Mental Disorders, fourth edition criteria for current or past psychiatric disorders, and all were physically healthy. In addition, the health status of all volunteers was confirmed by contacting their general practitioners. Family history of depressive disorder was determined by interviewing the participant and the relative's psychiatric history was confirmed from the relative themselves and/or the relative's general practitioner. The role of family history of depression in the co-distribution of serotonergic markers will be reported separately. The study recruited volunteers from two sites in

Cambridge and Oxford, UK, and all participants underwent scans at Hammersmith Hospital in London. This study was approved by the local Research Ethics Committees at Cambridge, Oxford and the Hammersmith Hospital, London; and the Administration of Radioactive Substances Advisory Committee, UK. All subjects gave written informed consent.

Data Acquisition

Each subject had two PET scans one each using [11C] WAY-100635and [11C] DASB, and a T1-weighted magnetic resonance scan for brain structural information. The time interval between the PET scans was about 1 week and the order was not fixed. The PET data were acquired on a high-sensitivity ECAT EXACT3D (Siemens/CTI, Knoxville, TN, USA) scanner with an axial field of view of 23.4 cm and 95 reconstructed transaxial image planes (Spinks et al, 2000).

The mean spatial resolution is 4.8 ± 0.2 mm FWHM (transaxial, 1 cm off-axis) and 5.6 ± 0.5 mm (axial, on-axis). A 5 min transmission scan (with a [137]-Cs rotating point source) was performed before each emission scans for scatter and attenuation correction (Watson et al, 1996).

DASB

[11C] DASB was synthesized as described earlier through the reaction of [11C]methyliodide with the desmethyl precursor (Wilson et al, 2000). Both the DASB and the precursor desmethyl DASB were supplied by the Target Molecules (Southampton, UK). [11C] DASB was administered via injection into an antecubital vein as a smooth bolus over 30 s. The injected radioactivity was between 432.16 and 541.79 MBq (mean 495.43 MBq, SD 16.45 MBq). The radiochemical purity of the injected [11C] DASB was high and ranged from 95 to 100% (mean 97.58%, SD 1.40%). The dynamic PET data were acquired over 90 min in list-mode and were then re-binned post-acquisition into a series of 28 frames of increasing lengths.

WAY-100635

[11C] WAY-100635 was synthesized by GE healthcare, MRC-Clinical Sciences Centre by a remotely controlled production process using [11C] carboxylation of an immobilized Gringard reagent as described previously (McCarron et al, 1996).

Dynamic PET data were acquired over 95 min in list-mode setting, collecting 23 time frames over 95 min. A bolus injection of [11C] WAY-100635 between 237.12 and 313.33 MBq (mean 300.63 MBq, SD 11.49 MBq) was administered intravenously over 30 s into an antecubital fossa vein. Further details of the scanning protocol used at the Unit have been previously described (Bhagwagar et al, 2007; Hinz et al, 2008).

Magnetic Resonance Imaging

It was not possible to acquire all the magnetic resonance imaging (MRI) data on the same scanner because of technical problems and de-commissioning of scanners during the study. Consequently the MRI was performed on scanners

with a field strength of 0.5 T (0.5 Apollo system, Marconi Medical Systems, Cleveland, OH, USA; (TR = 30 ms, TE = 3 ms, flip angle = 30°, NSA = 1, voxel dimensions 0.98 × 1.65 × 1.6 mm³), 1.5 T (1.5 Eclipse system, Marconi Medical Systems, Cleveland, OH, USA; (TR = 30 ms, TE = 3 ms, flip angle = 30°, NSA = 1, voxel dimensions 0.98 × 1.6 × 1.6 mm³), or 3 T (3 T Intera Philips Medical Systems; (TR = 9.6 ms, TE = 4.6 ms, flip angle = 8°, NSA = 1, voxel dimensions 0.94 × 0.94 × 1.2 mm³). The scans (0.5 T MRI—9 subjects; 1.5 T MRI—17 subjects, and 3 T MRI—16 subjects) were all examined by an independent clinical neuroradiologist for abnormalities. No participants were excluded on the basis of this examination.

Defining Volume of Interest

MRI images were resliced (1 × 1 × 1 mm³) and co-registered to the corresponding subject's summed PET image (9–90 min for DASB; 9–95 min for WAY-100635) using a normalized mutual information method, which implements a rigid body (six parameters) transformation using SPM5 (http://www.fil.ion.ucl.ac.uk/spm) to give individual co-registered MRI images. The following regions of interest (ROI) were investigated for both ligands: hippocampus, amygdala, anterior medial temporal lobe, anterior lateral temporal lobe, parahippocampus, superior temporal gyrus, medial inferior temporal gyrus, posterior temporal lobe, insula, anterior cingulate cortex, posterior cingulate cortex, parietal lobe, occipital lobe, orbitofrontal gyrus, precentral gyrus, inferior frontal gyrus, medial frontal gyrus, superior frontal gyrus, and raphe nucleus. In addition the brainstem, caudate nucleus, putamen, thalamus, and globus pallidus were investigated for DASB scans. All regions except raphe were defined on a probabilistic atlas. Raphe was drawn manually by an expert neuroradiologist (Rabiner et al, 2002) and the region used for both ligands was identical for each participant. This atlas has been shown to have high reliability for these regions (Hammers et al, 2002, 2003) and the raphe region was validated using four independents images, assessed by the same blinded rater. The variability (difference/mean) for V_T and BP_{ND} (see below for definition of these measurements) was 6.6% and 7.8%, respectively. The SPM MNI T1 template was spatially normalized to the co-registered individual MRI image and the deformation parameters applied to the probabilistic atlas to delineate the ROIs on the individual co-registered MRI. This normalized atlas was resliced to dimensions of the PET images and segmented to obtain the activity from the gray matter only and for the cerebellum ROI delineation the vermis was excluded.

Generation of Plasma Input Function

For accurate quantification of the highly selective radiotracers selected for this study, we used arterial blood sampling as this was recommended for [11C] WAY-100635 (Parsey et al, 2000) and [11C] DASB (Frankle et al, 2006). For both the ligands, a plasma metabolite-corrected input function was generated and the delay of the arrival of the tracers in the ROIs relative to the brain was determined. The details of the protocols are described in detail elsewhere (Gunn et al, 2000; Hinz et al, 2008; Hinz and Turkheimer, 2006).

DASB Data Quantification

Graphical analysis of reversible radioligand binding together with the metabolite-corrected plasma input function was used to quantify the [11C] DASB binding in brain tissue relative to the radioligand concentration in arterial plasma. Regional estimates of the total volume of distribution (V_T) were obtained from the slope of the linear part of the plot (Logan, 1990). Parameters such as the threshold for the graphical analysis $t^* = 35$ min were set as previously optimized for [11C] DASB (Hinz et al, 2008).

The following equation was then applied to calculate the binding potential (BP_{ND}) relative to nondisplaceable uptake:

$$BP_{ND} = (V_T^{\text{Target Region}} - V_T^{\text{Cerebellum}})/V_T^{\text{Cerebellum}}$$

Cerebellar gray matter was used as a reference region because of comparatively low density of 5-HTT (Kish et al, 2005). To avoid the spillover from the occipital cortex, the reference region was carefully delineated in cerebellar gray matter with five to eight slices included leaving a margin of several millimeters to the outer borders of the cerebellum (Hirvonen et al, 2006; Parsey et al, 2000).

WAY Data Quantification

Quantitative tracer kinetic modelling of [11C] WAY-100635 was performed using two-tissue compartmental model with metabolite-corrected plasma input assuming that labelled metabolites did not cross the blood–brain barrier. Details of the model were elaborated by Innis et al (2007), and Parsey et al (2000) showed that the derivation of BP_{ND} by kinetic analysis using the arterial plasma input function appeared as the method of choice because of its higher test–retest reproducibility, lower vulnerability to experimental noise, and absence of bias in comparison with BP_{ND} estimates derived with the simplified reference tissue model.

Genotyping

A total of 40 participants were genotyped for the insertion/deletion polymorphism located proximal to the transcription initiation site of the 5-HTT-coding region (5-HTTLPR) as described previously (David et al, 2005). Because of logistic reason we did not manage to genotype the remaining two subjects.

The 5HTTLPR and rs25531 were genotyped according to the protocol by De Luca et al (2005).

Statistics

Correlational analyses were performed using Pearson's product moment correlation coefficient. In order to minimize false-positive correlations, we first excluded ROIs with a mean BP_{ND} lower than 0.5 and second applied appropriate multiple comparisons correction. This resulted in the inclusion of the following ROIs for DASB BP_{ND}: hippocampus, amygdala, anterior medial temporal lobe, anterior lateral temporal lobe, parahippocampus, superior temporal

gyrus, insula, anterior cingulate cortex, posterior cingulate cortex, orbitofrontal gyrus, inferior frontal gyrus, and raphe nucleus. No regions were excluded for WAY-100635 BP_{ND}. On the basis of previous studies and the known organization of the serotonergic system we present three sets of analyses: first, the relationships between WAY-100635 BP_{ND} and DASB BP_{ND} within the raphe nucleus (Lundberg *et al*, 2007) and the predefined ROIs; second, the relationships between raphe nucleus WAY-100635 BP_{ND} and DASB BP_{ND} across the rest of the brain and finally the relationships between raphe nucleus DASB BP_{ND} and WAY-100635 BP_{ND} across the rest of the brain. To control the family-wise error rate at the $\alpha = 0.05$, the set of *p*-values derived from the correlation analyses was corrected using the Hochberg procedure for multiple comparison compounded by the p-plot estimator of the number of true-null hypotheses (Turkheimer *et al*, 2001). Age, sex, genotype, and daylight minutes have been included as covariates in the analysis and these factors did not affect the significance of the correlations in this data set. In addition, we used principal component analysis to obtain a summary 'global' measure of BP_{ND} across the predefined anatomical ROIs to conduct linear, and 2nd and 3rd order polynomial regression analyses. All data were analyzed in SPSS for Windows version 17.0 (SPSS).

RESULTS

The mean BP_{ND} for WAY-100635 and DASB across the predefined ROIs is shown in Table 1.

Correlations between WAY-100635 and DASB BP_{ND}

For the entire sample of volunteers there was a significant relationship between DASB BP_{ND} and WAY-100635 BP_{ND} in the raphe nucleus ($r = 0.31$, $p = 0.045$), although this was no longer significant when partialling out the effect of family history of depression. This appears to be due to those with a family history of depression having higher DASB BP_{ND} values when the WAY-100635 BP_{ND} is higher, although this effect only tended toward significance (MANOVA $F_{2, 39} = 2.77$, $p = 0.075$). For the rest of the brain there were no further statistically significant intra-regional correlations between DASB BP_{ND} and WAY-100635 BP_{ND} ($Ps > 0.34$). The global summary measures across all regions (excluding raphe nucleus) for DASB BP_{ND} and WAY-100635 BP_{ND} were also not significantly related using linear, 2nd or 3rd order polynomial curve estimation ($Ps > 0.70$).

When we specifically tested the relationship between the raphe WAY-100635 BP_{ND} and DASB BP_{ND} across the brain 6 out of 16 regions showed a significant positive correlation at $p < 0.05$. This is illustrated within the correlation matrix shown in Figure 1. Two regions survived correction for multiple comparisons (Turkheimer *et al*, 2001): the insula ($r = 0.41$, p(corr) $= 0.03$) and superior temporal gyrus ($r = 0.40$, p(corr) $= 0.04$); see Figure 2. The inferior frontal gyrus showed a trend toward statistical significance ($r = 0.39$, p(corr) $= 0.053$). Including family history of depression status as a covariate in the analysis does not alter these findings. There was a trend toward a significant relationship between raphe WAY-100635 BP_{ND} and the global summary measure for DASB BP_{ND} for both linear

Table 1 The BP_{ND} Values of each ROI are Presented in the Table (mean ± SD)

Region	WAY BP_{ND} (mean ± SD)	DASB BP_{ND} (mean ± SD)	Ratio BP_{ND} (WAY BP_{ND}/DASB BP_{ND})
Hippocampus	6.24 ± 1.15	1.02 ± 0.19	6.13
Amygdala	5.50 ± 0.85	1.93 ± 0.42	2.84
Anterior medial temporal	5.17 ± 0.91	0.73 ± 0.19	7.05
Anterior lateral temporal	5.13 ± 0.99	0.51 ± 0.15	10.00
Parahippocampus	5.94 ± 0.93	0.78 ± 0.18	7.63
Superior temporal gyrus	5.11 ± 0.86	0.67 ± 0.14	7.66
Insula	5.81 ± 0.97	1.22 ± 0.21	4.75
Anterior cingulate	5.16 ± 0.85	0.86 ± 0.19	6.00
Posterior cingulate	3.78 ± 0.75	0.76 ± 0.18	4.98
Orbitofrontal	4.70 ± 0.85	0.57 ± 0.21	8.19
Gyrus frontoinferior	4.06 ± 0.69	0.53 ± 0.15	7.59
Raphe	3.31 ± 0.70	4.28 ± 1.14	0.77
Brainstem	—	1.73 ± 0.39	NA
Caudate nucleus	—	1.55 ± 0.35	NA
Putamen	—	2.18 ± 0.36	NA
Thalamus	—	1.95 ± 0.41	NA

Abbreviation: NA, not analyzed.

and quadratic models (r^2(linear) $= 0.089$, $p = 0.054$ and r^2(quadratic) $= 0.13$, $p = 0.071$). These values suggest that we cannot distinguish between these models. There were no statistically significant relationships between raphe DASB BP_{ND} and postsynaptic WAY-100635 BP_{ND} ($Ps > 0.10$).

Participants were classified on the basis of triallelic genotyping of the 5-HTTLPR where L-alleles were classified as either L_A or L_G. For the purposes of this analysis homozygotes $L_A L_A$ were coded as L' and L_G and all S-allele carriers were combined as S'. Participants were separated into L' ($n = 7$) and S'-carriers ($n = 33$; Nakamura *et al*, 2000; Hu *et al*, 2005; Zalsman *et al*, 2006). Similar to the whole group analysis there were no statistically significant intra-regional correlations between DASB BP_{ND} and WAY-100635 BP_{ND} in either of the genotypic groups. When we specifically tested the relationship between the raphe WAY-100635 BP_{ND} and DASB BP_{ND}, 6 out of 17 regions in the LL group showed a significant positive correlation at $p < 0.05$, overlapping with the regions from the total sample, but also including the anterior temporal lobes, parahippocampal gyrus, and putamen. None of these correlations survived multiple comparisons correction using the Hochberg procedure (Turkheimer *et al*, 2001), although the sample size may have limited our ability to detect significant changes.

The Effects of Age and 5-HTTLPR Allelic Variations on WAY-100635 and DASB BP

Age was inversely associated with WAY-100635 BP_{ND} in 9 out of 18 brain regions ($p < 0.05$) although none of these correlations survived multiple comparisons correction. Age was positively associated with DASB BP_{ND} in 2 out of 17
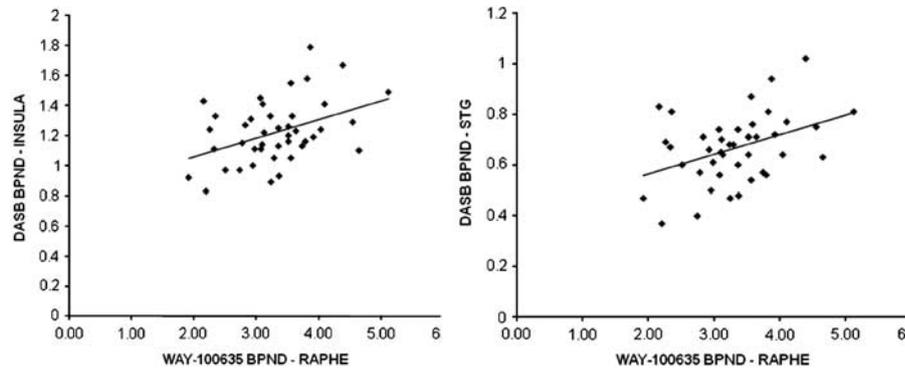
Figure 1 Scatter plot with regression line for dorsal raphe nucleus WAY-100635 BP_{ND} with DASB BP_{ND} in the insula (left panel, $r^2 = 0.17$) and superior temporal gyrus (right panel, $r^2 = 0.16$).
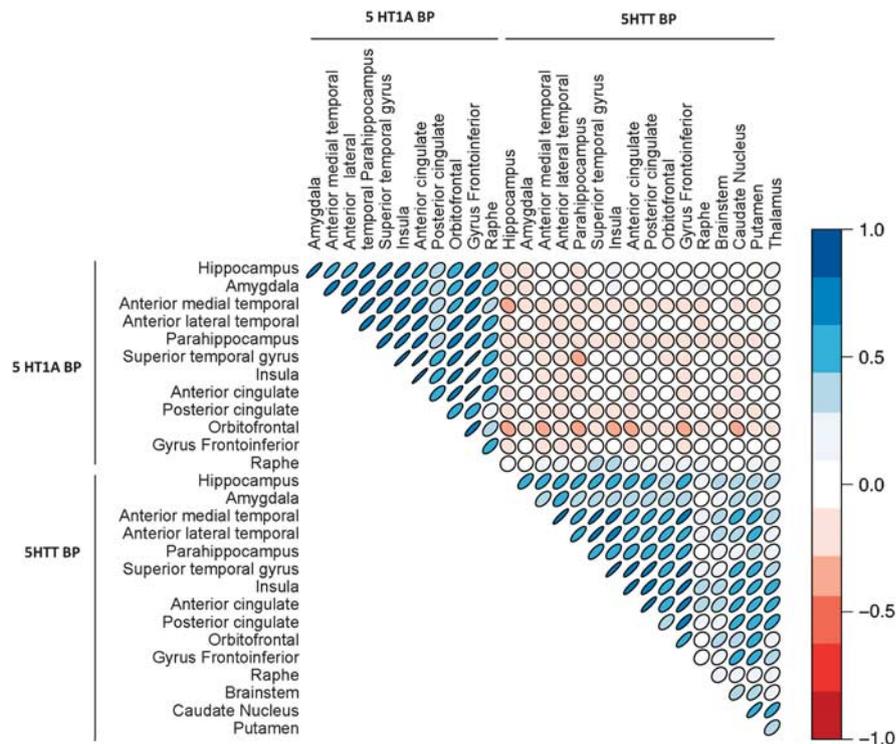
Figure 2 Regional correlation matrices between 5-HT1A BP_{ND} (measured with [11C] WAY-100635) and 5HTT BP_{ND} (measured with [11C] DASB). The shape, direction, and the color of the ellipses designate the magnitude and the direction of the correlation.

regions, and again none of these correlations survived multiple comparisons correction.

MANOVA was used to compare WAY-100635 *BP* and DASB *BP* between the 5-HTTLPR groups (with age as a covariate) for all regions. For WAY-100635 BP_{ND} there were no differences between 5-HTTLPR groups ($F_{19, 17} = 0.59$, $p = 0.87$). For DASB BP_{ND} was higher in the S′-carriers than the L′ group ($F_{24, 12} = 3.09$, $p = 0.023$), although the small number of participants in the L′ group ($n = 7$) compared with the S′-carriers makes it difficult to draw clear conclusions from this difference.

DISCUSSION

The main findings of the present study are that, in the largest sample reported to date, DRN WAY-100635 BP_{ND},

a putative index of serotonergic tone, was positively correlated with DASB BP_{ND} in insula, superior temporal gyrus, but not limbic regions (eg, amygdala and hippocampus); this relationship was not modulated by 5-HTTLPR variations.

We did not find support for our first hypothesis that lower 5-HTT densities in limbic regions will be accompanied by lower 5-HT1A receptor density in the same regions. This finding in a group of 42 volunteers clarifies the inconsistent results reported to date (Frey *et al*, 2008; Lundberg *et al*, 2007; Takano *et al*, 2008), which used smaller sample sizes of 8–14 volunteers. Thus, our results indicate that within limbic and cortical brain regions *in vivo* PET measurements of WAY-100635 BP_{ND} and DASB BP_{ND} appear to act as independent markers of serotonergic function. Within the raphe nucleus these two presynaptic

serotonergic markers were weakly related. This was not unexpected because both of these receptor subtypes in the DRN will be present in proportion with the number of 5-HT neurons. Intriguingly, controlling family history of depression reduced this correlation, because of the relatively higher conjoint BP_{ND} values for the two tracers, although this effect only tended toward significance. Whether the same effect is present in patients diagnosed with depression is not known.

Our data provide evidence that variations in DRN 5-HT1A receptor density can influence the density and/or function of other serotonin receptor subtypes. However, the precise causal pathway and etiology of this relationship cannot be determined from this data alone. On the one hand, reduced DRN 5-HT neuron firing (and presumably serotonergic tone) due to higher DRN 5-HT1A density might be predicted to be compensated for by reduced 5-HTT density at projection sites; this opposes our findings. Alternatively, we can speculate that 5-HT release, known to be dependent on burst firing of sub-populations of DRN 5-HT neurons (Gartside *et al*, 2000), determines 5-HTT density. The relationship between burst firing and 5-HT1A density is not currently known.

The relationship between DRN 5-HT1A density and insula, superior temporal and inferior frontal cortical 5-HTT may reflect serotonergic control of their known associations with specific aspects of emotional and executive processing. The insula cortex, which forms part of a so-called 'paralimbic' circuit is known to be important for the representation and monitoring of emotional states (Critchley *et al*, 2004), the superior temporal gyrus has been associated with the processing of both facial and other social stimuli (Habel *et al*, 2005; Ashwin *et al*, 2007; Barraclough *et al*, 2005) and the inferior frontal gyrus is important in impulsive behavior, which may be impaired in patients with depression. Indeed functionality within these regions is sensitive to serotonergic manipulations with SSRI administration (Smith *et al*, 2002; Anderson *et al*, 2007; Arce *et al*, 2008; Nemoto *et al*, 2003), and tryptophan depletion (Fusar-poli *et al*, 2007; Rubia *et al*, 2005). Although it is known that sub-populations of 5-HT neurons are present in the midbrain, their differential anatomical connectivity is not known. The regional differences in correlation may thus be due to 5-HT anatomical connectivity, for example, DRN axons contribute more to the serotonergic cortical innervations compared with the other midbrain nuclei (Hornung, 2003). However, our findings do not necessarily imply that 5-HT1A binding in the raphe nucleus cannot also influence limbic function. For example, Fisher *et al* (2006), combining PET and functional MRI measurements, showed 5-HT1A BP_{ND} in the DRN predicts amygdala activation to facial expressions of emotion.

Our findings may have relevance for understanding antidepressant action, although in the absence of supporting multi-ligand data following SSRI administration this must be considered as preliminary. It is generally accepted that the acute administration of SSRI increases synaptic 5-HT, which in turn activates 5-HT1A autoreceptors and reduces DRN firing (Hjorth *et al*, 2000). Recently, Richardson-Jones *et al* (2010) selectively knocked out raphe 5-HT1A autoreceptors without altering 5-HT1A

heteroreceptors in mice. They showed that mice expressing higher 5-HT1A autoreceptor levels when compared with lower 5-HT1A expressing mice had a reduced 5-HT response to acute administration of the antidepressant fluoxetine. They conclude that intrinsic autoreceptor levels and serotonergic tone before the onset of treatment are a critical aspect of antidepressant action. In addition, mice overexpressing 5-HTT in contrast to 5-HTT knockout mice have reduced extracellular 5-HT levels in many brain regions including cortex (Jennings *et al*, 2006). When taken together, these findings indicate that combined knowledge of 5-HTT and 5-HT1A autoreceptor density may have predictive value in understanding antidepressant response. Based on our preliminary findings in healthy volunteers, we speculate that patients with high 5-HTT density in the insula, superior temporal gyrus, and inferior frontal gyrus, when combined with high DRN 5-HT1A receptor density would be predicted to have a delayed response to SSRIs. This will need to be evaluated in future studies in patients with depressive disorders.

The potential role for genetic variations in, for example, transporter efficiency is poorly addressed in our sample because of the expected low number of those with L' genotype ($n = 7$) compared with the S'-carriers ($n = 33$). It is nonetheless intriguing to note that the strength of correlation observed, despite not reaching statistical significance, was greater in the smaller, L' group, which may align with the suggestion that this group have a more stable regulation of serotonin transmission (Kalbitzer *et al*, 2010).

These results contrast with the recently proposed inverted U-shaped relationship between 5-HT2A receptor density measured using [11C]altanserin and 5-HTT measured with [11C] DASB in a group of 46 volunteers (22 female; Erritzoe *et al*, 2010). The authors also predicted an inverted U-shaped relationship between 5-HT1A receptor density and 5-HTT in the hippocampus and frontal lobes. We were unable to support this prediction. However, unlike Erritzoe *et al* (2010), we included only male volunteers and it is possible that there may be gender differences in the 5-HTT and 5-HT1A correlations observed.

CONCLUSIONS

In a comparatively large sample of volunteers, we have shown that the relationship between 5-HT1A and 5-HTT PET indices was complex. We were unable to demonstrate robust, intra-regional relationships between 5-HT1A and 5-HTT densities. Inter-regionally, DRN 5-HT1A receptors were related to cortical (temporal and frontal regions) and paralimbic (insula), but not limbic 5-HTT. This latter finding may reflect differences in 5-HT tone between individuals, and highlights probable substrates sensitive to variations in DRN 5-HT function.

ACKNOWLEDGEMENTS

DISCLOSURE

REFERENCES

Abi-Dargham A (2007). Alterations in serotonin transmission in schizophrenia. *Int Rev Neurobiol* **78**: 133–164.

Alexandre C, Popa D, Fabre V, Bouali S, Venault P, Lesch K-P et al (2006). Early life blockade of 5-hydroxytryptamine 1A receptors normalizes sleep and depression-like behavior in adult knock-out mice lacking the serotonin transporter. *J Neurosci* **26**: 5554–5564.

Anderson IM, Del-Ben CM, McKie S, Richardson P, Williams SR, Elliott R et al (2007). Citalopram modulation of neuronal responses to aversive face emotions: a functional MRI study. *Neuroreport* **18**: 1351–1355.

Arce E, Simmons AN, Lovero KL, Stein MB, Paulus MP (2008). Escitalopram effects on insula and amygdala BOLD activation during emotional processing. *Psychopharmacology* **196**: 661–672.

Ashwin C, Baron-Cohen S, Wheelwright S, O'Riordan M, Bullmore ET (2007). Differential activation of the amygdala and the 'social brain' during fearful face-processing in Asperger Syndrome. *Neuropsychologia* **45**: 2–14.

Barnes NM, Sharp T (1999). A review of central 5-HT receptors and their function. *Neuropharmacology* **38**: 1083–1152.

Barraclough NE, Xiao D, Baker CI, Oram MW, Perrett DI (2005). Integration of visual and auditory information by superior temporal sulcus neurons responsive to the sight of actions. *J Cognitive Neuroscience* **17**: 377–391.

Bhagwagar Z, Murthy N, Selvaraj S, Hinz R, Taylor M, Fancy S et al (2007). 5-HTT binding in recovered depressed patients and healthy volunteers: a positron emission tomography study with [11C]DASB. *Am J Psychiatry* **164**: 1858–1865.

Cleare AJ, Messa C, Rabiner EA, Grasby PM (2005). Brain 5-HT1A receptor binding in chronic fatigue syndrome measured using positron emission tomography and [11C]WAY-100635. *Biol Psychiatry* **57**: 239–246.

Cowen PJ (2008). Serotonin and depression: pathophysiological mechanism or marketing myth? *Trends Pharmacol Sci* **29**: 433–436.

Critchley HD, Wiens S, Rotshtein P, Ohman A, Dolan RJ (2004). Neural systems supporting interoceptive awareness. *Nat Neurosci* **7**: 189–195.

David SP, Murthy NV, Rabiner EA, Munafó MR, Johnstone EC, Jacob R et al (2005). A functional genetic variation of the serotonin (5-HT) transporter affects 5-HT1A receptor binding in humans. *J Neurosci* **25**: 2586–2590.

De Luca V, Tharmalingam S, King N, Strauss J, Bulgin N, Kennedy J (2005). Association study of a novel functional polymorphism of the serotonin transporter gene in bipolar disorder and suicidal behaviour. *Psychopharmacology* **182**: 128–131.

Erritzoe D, Holst K, Frokjaer VG, Licht CL, Kalbitzer J, Nielsen FA et al (2010). A nonlinear relationship between cerebral serotonin transporter and 5-HT2A receptor binding: an *in vivo* molecular imaging study in humans. *J Neurosci* **30**: 3391–3397.

Fisher PM, Meltzer CC, Ziolko SK, Price JC, Moses-Kolko EL, Berga SL et al (2006). Capacity for 5-HT1A-mediated autoregulation predicts amygdala reactivity. *Nat Neurosci* **9**: 1362–1363.

Fox MA, Stein AR, French HT, Murphy DL (2010). Functional interactions between 5-HT(2A) and presynaptic 5-HT(1A) receptor-based responses in mice genetically deficient in the serotonin 5-HT transporter (SERT). *Br J Pharmacol* **159**: 879–887.

Frankle WG, Slifstein M, Gunn RN, Huang Y, Hwang D-R, Darr EA et al (2006). Estimation of serotonin transporter parameters with 11C-DASB in healthy humans: reproducibility and comparison of methods. *J Nucl Med* **47**: 815–826.

Frey BN, Rosa-Neto P, Lubarsky S, Diksic M (2008). Correlation between serotonin synthesis and 5-HT1A receptor binding in the living human brain: a combined [alpha]-[11C]MT and [18F]MPPF positron emission tomography study. *NeuroImage* **42**: 850–857.

Fusar-Poli P, Allen P, Lee F, Surguladze S, Tunstall N, Fu CHY et al (2007). Modulation of neural response to happy and sad faces by acute tryptophan depletion. *Psychopharmacology* **193**: 31–44.

Gartside SE, Hajo's-Korcsok E, Bagdy E, Harsing Jr LG, Sharp T, Hajo' M (2000). Neurochemical and electrophysiological studies on the functional significance of burst firing in serotonergic neurons. *Neuroscience* **98**: 295–300.

Geyer MA, Vollenweider FX (2008). Serotonin research: contributions to understanding psychoses. *Trends Pharmacol Sci* **29**: 445–453.

Gobbi G, Murphy DL, Lesch K, Blier P (2001). Modifications of the serotonergic system in mice lacking serotonin transporters: an *in vivo* electrophysiological study. *J Pharmacol Exp Ther* **296**: 987–995.

Gunn RN, Lammertsma AA, Grasby PM (2000). Quantitative analysis of [carbonyl-11C]WAY-100635 PET studies. *Nucl Med Biol* **27**: 477–482.

Habel U, Klein M, Kellermann T, Shah NJ, Schneider F (2005). Same or different? Neural correlates of happy and sad mood in healthy males. *NeuroImage* **26**: 206–214.

Hammers A, Allom R, Koepp MJ, Free SL, Myers R, Lemieux L et al (2003). Three-dimensional maximum probability atlas of the human brain, with particular reference to the temporal lobe. *Hum Brain Mapp* **19**: 224–247.

Hammers A, Koepp MJ, Free SL, Brett M, Richardson MP, Labbé C et al (2002). Implementation and application of a brain template for multiple volumes of interest. *Hum Brain Mapp* **15**: 165–174.

Hinz R, Selvaraj S, Murthy NV, Bhagwagar Z, Taylor M, Cowen PJ et al (2008). Effects of citalopram infusion on the serotonin transporter binding [11C] DASB in healthy controls. *J Cereb Blood Flow Metab* **28**: 1478–1490.

Hinz R, Turkheimer FE (2006). Determination of tracer arrival delay with spectral analysis. *IEEE Trans Nucl Sci* **53**: 212–219.

Hirvonen J, Kajander J, Allonen T, Oikonen V, Någren K, Hietala J (2006). Measurement of serotonin 5-HT1A receptor binding using positron emission tomography and [carbonyl-11C]WAY-100635–considerations on the validity of cerebellum as a reference region. *NeuroImage* **31**: T127–T128.

Hjorth S, Bengtsson HJ, Kullberg A, Carlzon D, Peilot H, Auerbach SB (2000). Serotonin autoreceptor function and antidepressant drug action. *J Psychopharmacol* **14**: 177–185.

Hornung J-P (2003). The human raphe nuclei and the serotonergic system. *J Chem Neuroanat* **26**: 331–343.

Hoyer D, Hannon JP, Martin GR (2002). Molecular, pharmacological and functional diversity of 5-HT receptors. *Pharmacol Biochem Behav* **71**: 533–554.

Hu X, Oroszi G, Chun J, Smith TL, Goldman D, Schuckit MA (2005). An expanded evaluation of the relationship of four alleles to the level of response to alcohol and the alcoholism risk. *Alcohol Clin Exp Res* **29**: 8–16.

Innis RB, Cunningham VJ, Delforge J, Fujita M, Gjedde A, Gunn RN et al (2007). Consensus nomenclature for *in vivo* imaging of reversibly binding radioligands. *J Cereb Blood Flow Metab* **27**: 1533–1539.

Jennings KA, Loder MK, Sheward WJ, Pei Q, Deacon RMJ, Benson MA et al (2006). Increased expression of the 5-HT

transcorter confers a low-anxiety phenotype linked to decreased 5-HT transmission. *J Neurosci* **26**: 8955–8964.

Kalbitzer J, Erritzoe D, Holst KK, Nielsen FA, Marner L, Lehel S et al (2010). Seasonal changes in brain serotonin transporter binding in short serotonin transporter linked polymorphic region-allele carriers but not in long-allele homozygotes. *Biol Psychiatry* **67**: 1033–1039.

Kish SJ, Furukawa Y, Chang L-J, Tong J, Ginovart N, Wilson A et al (2005). Regional distribution of serotonin transporter protein in postmortem human brain: is the cerebellum a SERT-free brain region? *Nucl Med Biol* **32**: 123–128.

Parsey RV, Slifstein M, Hwang D-R, Abi-Dargham A, Simpson N, Mawlawi O et al (2000). Validation and reproducibility of measurement of 5-HT1A receptor parameters with [carbonyl-11C]WAY-100635 in humans: comparison of arterial and reference tissue input functions. *J Cereb Blood Flow Metab* **20**: 1111–1133.

Li Q, Wichems C, Heils A, Lesch K-P, Murphy DL (2000). Reduction in the density and expression, but not G-Protein coupling, of serotonin receptors (5-HT1A) in 5-HT transporter knock-out mice: gender and brain region differences. *J Neurosci* **20**: 7888–7895.

Logan J, Fowler JS, Volkow ND, Wolf AP, Dewey SL, Schlyer DJ et al (1990). Graphical analysis of reversible radioligand binding from time-activity measurements applied to [N-^{11}C-methyl]-(-)-cocaine PET studies in human subjects. *J Cereb Blood Flow Metab* **10**: 740–747.

Lundberg J, Borg J, Halldin C, Farde L (2007). A PET study on regional coexpression of 5-HT1A receptors and 5-HTT in the human brain. *Psychopharmacology* **195**: 425–433.

Mannoury la Cour C, Boni C, Hanoun N, Lesch K-P, Hamon M, Lanfumey L (2001). Functional consequences of 5-ht transporter gene disruption on 5-HT1A receptor-mediated regulation of dorsal raphe and hippocampal cell activity. *J Neurosci* **21**: 2178–2185.

McCarron JA, Turton DR, Pike VW, Poole KG (1996). Remotely-controlled production of the 5-HT1A receptor radioligand, [carbonyl-11C]WAY-100635, via 11C-carboxylation of an immobilized Grignard reagent. *J Labelled Comp Radiopharm* **38**: 941–953.

Nakamura M, Ueno S, Sano A, Tanabe H (2000). The human serotonin transporter gene linked polymorphism (5-HTTLPR) shows ten novel allelic variants. *Mol Psychiatry* **5**: 32–38.

Nemoto H, Toda H, Nakajima T, Hosokawa S, Okada Y, Yamamoto K et al (2003). Fluvoxamine modulates pain sensation and affective processing of pain in human brain. *Neuroreport* **14**: 791–797.

Rabiner EA, Messa C, Sargent PA, Husted-Kjaer K, Montgomery A, Lawrence AD et al (2002). A database of [(11)C]WAY-100635 binding to 5-HT(1A) receptors in normal male volunteers: normative data and relationship to methodological, demographic, physiological, and behavioral variables. *Neuroimage* **15**: 620–632.

Richardson-Jones JW, Craige CP, Guiard BP, Stephen A, Metzger KL, Kung HF et al (2010). 5-HT1A autoreceptor levels determine vulnerability to stress and response to antidepressants. *Neuron* **65**: 40–52.

Rubia K, Lee F, Cleare AJ, Tunstall N, Fu CHY, Brammer M et al (2005). Tryptophan depletion reduces right inferior prefrontal activation during response inhibition in fast, event-related fMRI. *Psychopharmacology* **179**: 791–803.

Smith RL, Gresch PJ, Barrett RJ, Sanders-Bush E (2002). Stimulus generalization by fenfluramine in a quipazine-ketanserin drug discrimination is not dependent on indirect serotonin release. *Pharmacol Biochem Behav* **72**: 77–85.

Takano H, Ito H, Takahashi H, Arakawa R, Kodaka F, Sekine M et al (2008). A database of the intraindividual presynaptic serotonin transporter and postsynaptic serotonin 1A receptor functions: a PET study with [C-11]WAY-100635 and [C-11]DASB. *NeuroImage* **41**: T170.

Turkheimer FE, Smith CB, Schmidt K (2001). Estimation of the number of 'true' null hypotheses in multivariate analysis of neuroimaging data. *NeuroImage* **13**: 920–930.

Varnäs K, Halldin C, Hall H (2004). Autoradiographic distribution of serotonin transporters and receptor subtypes in human brain. *Hum Brain Mapp* **22**: 246–260.

Watson CC, Newport D, Casey ME (1996). A single scatter simulation technique for scatter correction in 3D PET. *Three-Dimensional Image Reconstr Radiol Nucl Med* **4**: 255–268.

Wilson AA, Ginovart N, Schmidt M, Meyer JH, Threlkeld PG, Houle S (2000). Novel radiotracers for imaging the serotonin transporter by positron emission tomography: synthesis, radio-synthesis, and in vitro and ex vivo evaluation of 11C-labeled 2-(Phenylthio)araalkylamines. *J Med Chem* **43**: 3103–3110.

Spinks TJ, Jones T, Bloomfield PM, Bailey DL, Miller M, Hogg D et al (2000). Characteristics of ECAT EXACT3D positron tomograph. *Phy Med Biol* **45**: 2601–2618.

Zalsman G, Huang Y-Y, Oquendo MA, Burke AK, Hu X-Z, Brent DA et al (2006). Association of a triallelic serotonin transporter gene promoter region (5-HTTLPR) polymorphism with stressful life events and severity of depression. *Am J Psychiatry* **163**: 1588–1593.